Impact of Border Enforcement Measures, Medical Resources, and Public Counter-Compliancy on the Global Spread of the Novel Covid-19: Two-Body Export-Importation Epidemic Dynamics

Authors

K M Ariful Kabir [a), b)], Atiqur Chowdhury [c)], Jun Tanimoto[a), d)]

a) Interdisciplinary Graduate School of Engineering Sciences, Kyushu University, Kasuga-koen, Kasuga-shi, Fukuoka 816-8580, Japan.

b) Department of Mathematics, Bangladesh University of Engineering and Technology, Dhaka, Bangladesh.

c) College of Business, Economics, Applied Statistics and International Business, MSC 3CQ, PO Box 30001, New Mexico State university, Las Cruces, NM 88003-8001, U.S.A.

d) Faculty of Engineering Sciences, Kyushu University, Kasuga-koen, Kasuga-shi, Fukuoka 816-8580, Japan.

Corresponding author

K M Ariful Kabir, k.ariful@yahoo.com, kmarifulmath@gmail.com

Abstract

In the wake of the novel coronavirus, SARS-CoV-19, the world has undergone a critical situation in which grave threats to global public health emerged. Among human populations across the planet, travel restraints, border enforcement measures, quarantine, and isolation provisions were implemented in an attempt to control and limit the spread of the contagion. Decisions on how to implement and enforce various control policies should be determined based on available real-world evidence and theoretical prediction. In this study, we propose a novel exportation- importation epidemic model associated with the quarantine and hospitalized-isolation policies by considering the two-body system: a source country of a contagious disease and a neighboring country that is initially disease-free. The model is first applied to the original COVID-19 data in China, Italy, and the Republic of Korea (ROK) and observed through consistent fitting results with equivalent goodness-of-fit. Then, the data are estimated per the fitting parameters. Driven by these parametric settings and considering the normalized population, the numerical analysis, and epidemiological exploration, this work further elucidates the substantial impact of quarantine policies, healthcare facilities, and the public counter-compliance effect.

Keywords

SARS-CoV-19, importation-exportation, healthcare facilities, public counter-compliancy.

Preprints (www.preprints.org) | NOT PEER-REVIEWED | Posted: 14 May 2020 doi:10.20944/preprints202005.0242.v1

Introduction

The novel coronavirus, termed SARS-CoV-2, incites the COVID-19 disease and is a serious endemic virus first found in Hubei, China, on December 31, 2019 [1–8]. Its rapid emergence and terrestrial diffusion caused major global concerns, as the world has seen 2.3 million confirmed cases with 0.16 million total deaths in the previous four months (January–April 2020) [9]. Yet, to date, no vaccination, preventive medication, or effective treatment against the disease exist. Nevertheless, researchers are working on the development of medicine, and few clinical trials are ongoing [10]. Further, the human mobility aspect plays a critical role in the spread of transmissible diseases by travelers from one region to another [11–14]. To mitigate the epidemic and preclude the persistence of the disease in the human population worldwide, some major prevention and incentive strategies were undertaken, such as social distancing, forced quarantine, rapid isolation, state emergency, strict lock-downs, and mobility restrictions [15,16]. Moreover, resistance against prevention policies, the role of global exportation- importation [17] on transmission, and medical resources can account for the spread of the disease. In this paper, a new export-importation SEIQJR (susceptible-exposed-infected-quarantine-isolation-removed) epidemic mathematical model is formulated to present the current COVID-19 situation by including mobility restrictions, medical resources, and public counter-compliant aspects.

A number of mathematical models with a compartmental mean-field approach were used to model the transmission dynamics of a novel coronavirus-carrying disease and to evaluate prevention policies for disease intervention. A theoretical epidemiological approach could contribute to analyzing real data, recognizing epidemic patterns, and estimating the uncertainty for the transmittable diseases. Recently, researchers incorporated the susceptible-exposed-infected-recovered (SEIR), or modified SEIR, epidemic-theoretical framework [18–21] into the dynamic analysis to further explore the incidence, control strategies, and tracing factors of the COVID-19 disease. Moreover, notable works include Arenas et al. [22] for their presentation of a spatiotemporal COVID-19 epidemic model, Teles et al. [23] for their representation of the evolution of COVID-19 in Portugal using an adaptive SIR model, Chen et al. [24], for their study of the time-dependent SIR mode, Xia et al. [25] for their study of the epidemic SEIR model in the Middle East and South Korea, and Canabarro et al. [26] for their success in establishing an age-structure COVID-19 model in Brazil.

As an active vaccine or treatment drug for CODIV-19 is not expected to become available for months to years, we must rely on commonly implemented control measures, such as isolation and quarantine policy. The term isolation has come to specify a period of separation in which human contact is minimal, and those under treatment, or self-isolation as carriers of the disease, refrain from spreading the infection to others. Conversely, quarantine can be defined as an enforced restriction of movement and physical separation of an individual who may have been exposed to a contagious disease. Previously, several mathematical epidemic models of the outbreak were used to evaluate the impact of isolation and quarantine on the spread of infectious diseases [27–29]. Recently, Alam et al. [30] extensively investigated the epidemic vaccination game model alongside isolation and quarantine policies in repeated seasons. Aside from the quarantine-isolation based all-purpose epidemic model, researchers focused on studying the theoretical epidemic model to control and predicting the infections trends of the novel COVID-19 by introducing isolation, quarantine, and treatment strategies [31, 32]. To identify quarantine and social-distancing schemes in developing countries, Chowdhury et al. [16] used a SEQIR model to describe the spread of the novel coronavirus. As cited above, quarantine policies can be a public-based control measure where the authorities enforce social isolation, regardless of the intention of each individual. Isolation can be said to be an ultimate remedy that depend on existing medical facilities/resources, such as testing-kits, ventilation, capacity, equipment, and medical staff. To implement a realistic isolation-quarantine based epidemic model for COVID-19, in the

Preprints (www.preprints.org) | NOT PEER-REVIEWED | Posted: 14 May 2020 doi:10.20944/preprints202005.0242.v1

present study, we presumed individual cooperation resistance against forced quarantine, as well as the limitations of medical resources that were commonly observed in the current situation.

The current nCoV-19 disease outbreak marks the highest emergence in the 21st century, as it demonstrated rapid global spread as a result of the prevalence of travel mobility [33, 34]. Traveling people can be responsible for the introduction and spread of infection to new areas, whether travel occurs at international levels through air or sea travel or at a more local level between different cities in the same county. Thus, understanding and restricting the spread of contagious disease through border control measures, such as airport screenings and travel restrictions, are pressing concerns when dealing with the risk of infection. To assess intricate human mobility as a whole, referred to above as a metapopulation migration aspect [35–40], we model the concept of the exportation- importation epidemic model, which can enumerate the spreading of infectious diseases via travelers. To understand the spread of COVID-19 from China to other countries, we chose Italy and the Republic of Korea (ROK) as the initially disease-free countries and China as the source country. We highlight the connected dynamics between an origin country and a neighboring country, although our general model presumes multi-neighboring countries. The two-body problem can provide a foundation for a complex multi-body problem without the loss of substances. We used day-to-day COVID-19 incidence data for China, Italy, and ROK, starting from January 22, 2020, to statistically estimate the parameter settings that correspond to our proposed export- importation SEIQJR epidemic model. As expected, we found a significant correlation between the real reported data and the simulated data of the global exportation- importation event for three countries. To make the analysis more profound and trackable, we presume the normalized population (the total population is 1) by supposing a well-mixed and infinitely large population described in previous works [41–43]. Motivated by the COVID-19 disease, the present mathematical epidemic model is the first to envision complex exportation-importation traveling dynamics by introducing quarantine and hospitalized-isolation control measures, which also explore the ideas of public counter-compliant factor and healthcare resources.

In this study, our focus is on the two-body problem in the spread of COVID-19, which relates to the interaction traffic between country A (epidemic origin) and country B (one of the neighboring countries). The timing of mutual traffic closing-down influences how COVID-19 spreads in country B, which is controlled by the parameter I_0. Moreover, we are concerned with whether the following aspects recognize the influence of the epidemic dynamics occurring in each country, depending on the local condition of each country: the number of people compliant with the government instructions on self-quarantine, how strongly the government imposes the self-quarantine instruction, and how adequate the government is in detecting infectious people who become isolated. Further, moving away from the real-word scenario, with China as country A and either Italy or the ROK as country B, we are concerned with the sensitivity of the study per the aforementioned focal point. In the sensitivity study below, we vary the focal parameters systematically so that the results be presented in a series of two-dimensional (2D) heat-maps.

Model and Method

General export- importation epidemic spreading model

A modified exportation-importation SEIR epidemic model is suggested to present the impact of travel, quarantine, hospitalized-isolation, medical resources, and public behavior toward government decisions, as well as uncover the trends of COVID-19 in various countries. To model the SEIR epidemic dynamic, a metapopulation for several groups (islands or countries), called subpopulations, was used. In each subpopulation, the population is divided into six compartments: susceptible (S_k), exposed (E_k), quarantined (Q_k), infected (I_k), hospitalized-isolation (J_k), and removed (R_k), where k represents the number of countries or subpopulation: k = 1, 2, 3,…, n, and n is the maximum number of subpopulations (Figure 1). The mean-field compartmental aspect is presumed to develop the theoretical system inside each subpopulation for SEIQJR, in which traveling and mobility are only permitted for those who are susceptible

Preprints (www.preprints.org) | NOT PEER-REVIEWED | Posted: 14 May 2020 doi:10.20944/preprints202005.0242.v1

or exposed. We begin with the so-called mean-field approximation method for $n-$ subpopulations that can be inscribed as a set of non-linear dynamic equations:

$$\dot{S}_k = -\beta_k S_k(I_k + q_k Q_k) - m_k S_k + \sum_{j \neq k}^{n} m_j S_j \tag{1.1}$$

$$\dot{E}_k = \beta_k S_k(I_k + q_k Q_k) - \alpha_k E_k - \mu_k E_k + \sum_{j \neq k}^{n} \mu_j E_j \tag{1.2}$$

$$\dot{I}_k = \alpha_k(1 - \eta_k)E_k - (\gamma_k + r_k + d_k)I_k \tag{1.3}$$

$$\dot{Q}_k = \alpha_k \eta_k E_k - \delta_k Q_k \tag{1.4}$$

$$\dot{J}_k = r_k I_k - w_k J_k \tag{1.5}$$

$$\dot{R}_k = \delta_k Q_k + \gamma_k I_k + d_k I_k + w_k J_k \tag{1.6}$$

The model described above defines a set of population compartments in $n-$ subpopulations. A susceptible individual can be exposed through active contact with an infected person and a quarantined person at the contact rate β_k. Further, we used $q_k \epsilon [0,1]$ to define the public counter-compliant factor, and 0 (zero) reflects all people of respective countries who are supportive of government instruction by self-isolating. However, 1 implies the worst-case situation in which quarantine is nominal. Moreover, an exposed person can be considered a suspected person, or a low-level virus carrier, as they may be otherwise healthy while still harboring and transmitting the infection. The transition rate of exposed to infected individuals and exposed to quarantined individuals are denoted by $\alpha_k(1 - \eta_k)$ and $\alpha_k \eta_k$, respectively. Here, the proportion of becoming quarantined is denoted by η_k, which stipulates how many exposed individuals assumed the quarantine policy declared by the government. The proportion of non-quarantined exposed individuals who become infected is reflected as $1 - \eta_k$. Quarantined individuals stay home, in safe places, or are forcefully removed from contact with those who were suspected and were not tested or treated. An infected person is symptomatic and tested positive for the COVID-19 disease, whereas an isolated person is hospitalized and denoted by J. Such a person is under medical-custody to restrict contact with those susceptible to the disease. The testing rate, diagnostic rate, or transferring rate of infected individuals to receive hospitalized-isolation is denoted by the isolation rate as r_k, which relies on available medical resources, indicated by J_0. Finally, a recovered individual is either coming from the natural recovery process (from I), quarantine (from Q), or hospitalized-isolation (from J). The recovery period for compartments infected, quarantined, and hospitalized-isolation are symbolized by $1/\gamma_k$, $1/\delta_k$, and $1/w_k$, respectively, and the parameter d_k indicates the COVID-19 death rate. The compartment R represents recovered or removed individuals. In order to perform the exportation-importation epidemic model, we presumed a constant mobility rate m_k from the susceptible (in country A) to susceptible (in country B) moving and the conditional μ_k from the exposed (in country A) to exposed (in country B) traveling and vis-a-vis.

Basic reproduction number, R_0:

Based on the equations of our model (equations 1.1–1.6), we can determine the disease-free equilibrium point as $(P_k; 0; 0; 0; 0)$, where the variables are organized in the same way as the equation in the system. For each country, we supposed certain conditions: $S_k(0) = P_k$, $m_k \cong 0$, and $\mu_k \cong 0$, where P_k implies the total number of population in k^{th} country $(k = 1, 2, 3, \dots N.)$.
The disease-free equilibrium leads to the following matrices F and V:

Preprints (www.preprints.org) | NOT PEER-REVIEWED | Posted: 14 May 2020 doi:10.20944/preprints202005.0242.v1

$$F = \begin{bmatrix} 0 & P_k\beta_k & P_k\beta_k q_k & 0 \\ 0 & 0 & 0 & 0 \\ 0 & 0 & 0 & 0 \\ 0 & 0 & 0 & 0 \end{bmatrix} \qquad V = \begin{bmatrix} \alpha_k & 0 & 0 & 0 \\ -\alpha_k(1-\eta_k) & r_k+\gamma_k+d_k & 0 & 0 \\ -\alpha_k\eta_k & 0 & \delta_k & 0 \\ 0 & -r_k & 0 & w_k+d_k \end{bmatrix} \tag{2.1}$$

The invert of V yields:

$$V^{-1} = \begin{bmatrix} \frac{1}{\alpha_k} & 0 & 0 & 0 \\ \frac{(1-\eta_k)}{r_k+\gamma_k+d_k} & \frac{1}{r_k+\gamma_k+d_k} & 0 & 0 \\ \frac{\eta_k}{\delta_k} & 0 & \frac{1}{\delta_k} & 0 \\ \frac{r_k(1-\eta_k)}{(r_k+\gamma_k+d_k)(w_k+d_k)} & \frac{r_k}{(r_k+\gamma_k+d_k)(w_k+d_k)} & 0 & \frac{r_k}{(r_k+\gamma_k+d_k)(w_k+d_k)} \end{bmatrix} \tag{2.2}$$

The next-generation matrix is given by:

$$FV^{-1} = \begin{bmatrix} \frac{P_k\beta_k(1-\eta_k)}{r_k+\gamma_k+d_k} + \frac{P_k\beta_k q_k\eta_k}{\delta_k} & \frac{P_k\beta_k}{r_k+\gamma_k+d_k} & \frac{P_k\beta_k q_k}{\delta_k} & 0 \\ 0 & 0 & 0 & 0 \\ 0 & 0 & 0 & 0 \\ 0 & 0 & 0 & 0 \end{bmatrix} \tag{2.3}$$

Thus, the basic reproduction number R_0 is the spectral radius $\rho(FV^{-1})$ as follows:

$$R_0^k = \frac{P_k\beta_k\left(\left((r_k+\gamma_k+d_k)q_k-\delta_k\right)\eta_k+\delta_k\right)}{(r_k+\gamma_k+d_k)\delta_k}; k = 1,2,3,\dots,n. \tag{3}$$

The stability of the system can be concluded by the following theorem.

Theorem: (i) If $R_0^k \leq 1$, the disease-free equilibrium is locally stable. (ii) If $R_0^k > 1$, the disease-free equilibrium is unstable.

Two-body export- importation epidemic spreading model

To explore the proposed exportation-importation SEQIJR epidemic model for COVID-19, we consider the two-body epidemic system: country A and country B ($n = 2$), defined by:

Country A:

$$\dot{S}_1 = -\beta_1 S_1(I_1 + q_1 Q_1) + q_1 S_1 - q_2 S_2 \tag{4.1}$$

$$\dot{E}_1 = \beta_1 S_1(I_1 + q_1 Q_1) - \alpha_1 E_1 + \mu_1 E_1 - \mu_2 E_2 \tag{4.2}$$

Preprints (www.preprints.org) | NOT PEER-REVIEWED | Posted: 14 May 2020 doi:10.20944/preprints202005.0242.v1

$$\dot{I}_1 = \alpha_1(1-\eta_1)E_1 - (\gamma_1 + r_1 + d_1)I_1 \quad (4.3)$$

$$\dot{Q}_1 = \alpha_1\eta_1 E_1 - \delta_1 Q_1 \quad (4.4)$$

$$\dot{J}_1 = r_1 I_1 - w_1 J_1 \quad (4.5)$$

$$\dot{R}_1 = \delta_1 Q_1 + \gamma_1 I_1 + d_1 I_1 + w_1 J_1 \quad (4.6)$$

Country B:

$$\dot{S}_2 = -\beta_2 S_2(I_2 + q_2 Q_2) - m_1 S_1 + m_2 S_2 \quad (5.1)$$

$$\dot{E}_2 = \beta_2 S_2(I_2 + q_2 Q_2) - \alpha_2 E_2 - \mu_1 E_1 + \mu_2 E_2 \quad (5.2)$$

$$\dot{I}_2 = \alpha_2(1-\eta_2)E_2 - (\gamma_2 + r_2 + d_2)I_2 \quad (5.3)$$

$$\dot{Q}_2 = \alpha_2\eta_2 E_2 - \delta_2 Q_2 \quad (5.4)$$

$$\dot{J}_2 = r_2 I_2 - w_2 J_2 \quad (5.5)$$

$$\dot{R}_2 = \delta_2 Q_2 + \gamma_2 I_2 + d_2 I_2 + w_2 J_2 \quad (5.6)$$

The first sub-model, country A, applies to those that live in the epidemic originating county, whereas the second sub-model, country B, indicates individuals that live in an initially disease-free country. Meanwhile, the term importation refers to a traveler who lives in a disease-free country and then visited an endemic country, only to return carrying the infection and potentially introducing the disease to their disease-free country. The term exportation indicates the situation where individuals residing in an epidemic country travel to a disease-free country, where they could also introduce the infection in the visited disease-free country. In both scenarios, susceptible and exposed individuals are permitted to travel randomly from one country to another. Moreover, the exposed individuals could be in a latent stage (asymptomic) and trigger disease outbreaks in disease-free regions.

Mobility and isolation rate

In the current exportation-importation framework, we can classify two types of bidirectional mobility in terms of moving individuals from susceptible (Country A/B) to susceptible (Country B/A) and exposed (Country A/B) to exposed (Country B/A) state as $\mu_*(=\mu_1=\mu_2 \ldots = \mu_n)$ and $m_*(=m_1=m_2 \ldots \ldots = m_n)$, respectively. In the present study, we assume that the susceptible and exposed people who travel always follow a binary decision aspect, defined as:

$$\mu_* = \begin{cases} \mu_0 & if\ I_1(t) < I_0 \\ 0 & otherwise \end{cases} \quad (6.1)$$

$$m_* = \begin{cases} m_0 & if\ I_1(t) < I_0 \\ 0 & otherwise \end{cases} \quad (6.2)$$

Here, the mobility rate (μ_*, m_*) satisfies the inequality $I_1(t) < I_0$, indicating that the individual cannot be allowed to travel (due to mobility restrictions) if the number of infected cases remaining in the country of origin reached or overflowed at certain threshold values, I_0.

To evaluate the clinical demand and hospital capacity against epidemic spreading, we presume the conditional isolation rate r_k, defined as:

Preprints (www.preprints.org) | NOT PEER-REVIEWED | Posted: 14 May 2020 doi:10.20944/preprints202005.0242.v1

$$r_k = \begin{cases} r_0 & if\ J_k(t) < J_0 \\ 0 & otherwise \end{cases} \quad (7)$$

where r_0 is the constant transmission rate that the infected individuals, who were confirmed to be highly infected, become isolated or hospitalized, depending on hospital capacity, which is denoted by J_0. Therefore, $J_k(t) < J_0$. However, if the hospitals are overcrowded, some of those individuals would be temporarily delayed from entering the hospital due to a lack of vacancies ($J_0 = 0$).

Parameter estimation and prediction

In order to estimate the parameter setting, to perform the fitting, we use the daily original COVID-19 positive case data for China, Italy, and the ROK from January 22, 2020, to March 31, 2020 [9]. A linear regression polynomial fit technique is used to evaluate the parameter values. This parameter identification process premises that each of the focal countries is stand-alone, meaning $\mu_0 = m_0 = 0$. Mobility less-significantly influences the identification of the global model parameters for each country as long as an appropriate initial infectious number is assumed. Figure 2 displays the comparison between the reported cases with the numerically simulated results for China (panel A), the ROK (panel B), and Italy (panel C). The estimated parameter values for the three countries are presented in Table 1. Here, P_k denotes the total population in each country. The linear regression analysis suggests that our model fit well compared with the reported cases with adjusted R^2 values for China ($R^2 = 0.3470$), Italy ($R^2 = 0.9594$), and the ROK ($R^2 = 0.8749$) (see Appendix). Thus, we demonstrate approximately 34%, 96%, and 87% accuracy to track the original confirmed COVID-19 cases for China, Italy, and ROK, respectively. However, due to a jump observed in China's data on the 20th day, the level of accuracy indicates unsatisfactory results.

Table 1: Estimated parameters for the SEIQJR epidemic model for China, Italy, and the Republic of South Korea except for the total population.

Parameter	Description	China	Italy	ROK
P_k	Total population	1.2301×10^9	3.0481×10^8	4.1260×10^8
β_k	Transmissibility rate	2.1231×10^{-9}	4.4271×10^{-8}	2.5113×10^{-8}
q_k	Public counter-compliant factor	1.0	0.9	0.9
α_k	Incubation rate to be infective	1.0	0.28	0.81429
η_k	Forced quarantine rate	0.5	0.25	0.5
γ_k	Recovery rate (natural)	0.1	0.45	0.1
r_k	Incubation rate to be isolation	0.02	0.02	0.02
δ_k	Recovery rate after quarantine	0.01	0.1	0.1
w_k	Recovery rate after isolation	0.02	0.02	0.02
d_k	Death rate	0.07	0.38	0.07

Normalized settings

In our export-importation SEIQJR epidemic model, the total population is divided into two subpopulations, country A and country B. If the total human population for country A and B are P_1 and P_2, respectively, and remain constant, then we presume that the total population of the epidemic system is $P_1 + P_2 = 1$, and the rate change of total human populations is zero. The normalized system of the dynamical model is obtained from equations (4 & 5) by dividing the total population $P_1 + P_2$, where $S_1(t) + E_1(t) + I_1(t) + Q_1(t) + J_1(t) + R_1(t) = P_1$ and $S_2(t) + E_2(t) + I_2(t) + Q_2(t) + J_2(t) + R_2(t) = P_2$. Using all the assumptions, including a basic reproduction number formulated in equation (3) and Table 1, we estimated the set of values for infinite and normalized dynamical systems, as summarized in Table 2.

Preprints (www.preprints.org) | NOT PEER-REVIEWED | Posted: 14 May 2020 doi:10.20944/preprints202005.0242.v1

Table 2: Parameters of the normalized epidemic dynamics and their estimations for country A and country B.

Parameter	Description	Country A (China)	Country B (Italy)
P_k	Total population	0.6	0.4
β_k	Transmissibility rate	2.612	3.39
q_k	Public counter-compliant factor	1.0 (Varied)	0.9 (Varied)
α_k	Incubation rate to be infective	1.0	0.28
η_k	Forced quarantine rate	0.5 (Varied)	0.25 (Varied)
γ_k	Recovery rate (natural)	0.1	0.45
r_k	Incubation rate to be isolation	0.02 (Varied)	0.02 (Varied)
δ_k	Recovery rate after quarantine	0.01	0.1
w_k	Recovery rate after isolation	0.02	0.02
d_k	Death rate	0.07	0.38

Numerical procedure

To numerically solve the impact of the implemented model stated in equations (4–7), we used the explicit finite difference method. Initially, we assumed the initial conditions for all simulations as $S_1(0) = P_1 = 0.6$, $E_1(0) = \cong 0(0.00001)$, $I_1(0) \cong 0(0.00001)$, $Q_1(0) = 0$, $J_1(0) = 0$, and $R_1(0) = 0$ for country A and $S_2(0) = P_2 = 0.4$, $E_2(0) = 0$, $I_2(0) = 0$, $Q_2(0) = 0$, $J_2(0) = 0$, and $R_2(0) = 0$ for country B. The parameters used are taken from Table 2, which defined as a default where setting countries A and B are reflected for the estimated parameters coming from evaluated values for China and Italy (Table 1). We know the [9] actual population fractions of China and Italy are not 0.6 and 0.4. The following exploration presumes that for two hypothetical countries (country A and country B), our focus is to quantify the sensitivity per the following parameters. Although we do not show detail, we confirmed that the population fraction does not exhibit significant sensitivity to the results obtained below. Unlike the fixed constant parameters, throughout our numerical experiments, we presumed the public counter-compliant factor (q_k), force quarantine rate (η_k), and incubation rate to be hospitalized-isolation (r_k) as the controlling parameters. Also, in the present study, we presumed the mobility rate as $\mu_0 = m_0 = 0.00001$.

Results and discussion

Time series analysis

To explore the impact of government enforcement, disease prevalence, public perception, and healthcare facilities on the epidemic dynamics of COVID-19, we used an exportation-importation SEIQJR compartmental model and performed a time series simulation according to three key parameters: forced quarantine rate (panel A), η, public counter-compliant factor (panel B), q, and incubation rate to be isolated or isolation rate (panel C), r, as seen in Figure 3. The baseline system values, defined as the default, for each of the parameters are taken from Table 2. While constructing the plots, we took $\eta_2 = 0.25$ (default), $\eta_2 = 0.1, \eta_2 = 0.5$, and $\eta_2 = 0.9$ for panel A; $q_2 = 0.9$ (default), $q_2 = 0.1$, and $q_2 = 0.5$ for panel B; and $r_2 = 0.02$ (default), $r_2 = 0.1$, and $r_2 = 0.5$ for panel C. In addition, sub-panels (a), (b), and (c) indicate the fraction of infected, quarantined, and hospitalized-isolation individuals, respectively. The set of graphs offered in Figure 3 demonstrates the three principal findings: (i) the rate of change in quarantine, η, inversely correlated with the fraction of the infected and hospitalized-isolation individuals, where increasing the values of η_2 reduces the number of infected as well as hospitalized individuals. Contrarily, the fraction of the quarantined population shows a positive association with η_2, which is natural. In general, a higher rate of quarantine impending from the governmental declaration or decree boosts the fraction of the quarantined population, which helps to reduce the disease spreading together with hospitalized-isolation.

Preprints (www.preprints.org) | NOT PEER-REVIEWED | Posted: 14 May 2020 doi:10.20944/preprints202005.0242.v1

(ii) A similar tendency exists between the rate of public counter-compliancy and infection prevalence observed that is among lower q_2 values, where infected densities are less. This phenomenon can be explained by the fact that people disobeyed orders to stay home and to avoid dense places for higher values of q_2. (iii) Finally, we found that the rate of change in incubation to hospitalized-isolation inversely linked with the fraction of infected and hospitalized-isolation densities. Indeed, the isolation rate, r_2, depends on the available resources or facilities of the healthcare system. Therefore, depending upon the parameter r_2, healthcare resources would be interesting to investigate. Taken together, these outcomes strongly suggest an interaction between the disease's prevalence and the impact of the controlling parameters of the normalized COVID-19 epidemic model.

Phase portrayed

To focus on the 2D phase diagrams, Figure 4 displays several phase portraits presenting the cumulative fraction of infected individuals in an epidemic season for (A) a default case (using Table 2), (B) the varying isolation acquired rate for country A, $r_1(= 0.3 \,\&\, 0.8)$, and (C) the varying isolation acquired rate for country B, $r_2(= 0.3 \,\&\, 0.8)$ in a steady-state position within the $(\eta, q)-$ parameter plane, i.e., $0 \leq \eta_1 = \eta_2 = \eta \leq 1{,}0 \leq q_1 = q_2 = q \leq 1$. Accordingly, sub-panels (a/a-*), (b/b-*), and (c/c-*), respectively, specify the full-scale phase portrayed by country A, country B, and the total of A + B deliberated under the varying parameters of r_1 (panel B) and r_2 (panel BC). Notably, all the presented phases portrayed the disease-free equilibrium for the zone colored in deep blue.

Figure 4(A) defined, as the default case elucidates, what occurs in both countries if we allow exposed mobility of those that are infected from country A (China) to country B (Italy) and the government-initiated quarantine practice to forcefully control the disease pandemic. First, we see that a higher η value reduces the number of infectious individuals, as it leads an individual to follow the quarantine policy to avoid disease transmission (white-dotted box in sub-panel (a) and (b)). Interestingly, country A (sub-panel (a)) displays no-sensitivity along q. This is due to the contribution from hospitalized-isolation controlled by r_1 being low, which keeps many people stay at the infected compartment (I); if a large number of incoming flux to infected is imposed (depending on η). Thus, relatively speaking, the sensitivity from q inevitably becomes smaller than that from η. As η directly controls the number of infected individuals, q is only able to indirectly control infected individuals. However, country B (sub-pane (b)) is unlike country A, demonstrating sensitivity to both directions. However, a q that is too high does not change color along q. Observing country B closely, we note that the condition with higher quarantine rates and less public counter-compliant factors function well and help to significantly to reduce the spread of the disease (white-dotted box and half-oval). This implies that if people are aware and cooperative in adhering to quarantine policy, a tendency towards reducing the spread of the disease is observed in the infected fraction of individuals (country B). Subsequently, observing the fraction of the total of A + B (infected individuals of country A+ country B) in sub-panel (c) shows a similar effect.

Then, we observed how the incubation rates to be isolated for country A, r_1 (Figure 4(B)) and country B, r_2 (Figure 4(C)) affect epidemic spreading and how that rate influences the $(\eta, q)-$ phase space. These two crucially important parameters were introduced here to show the impact of the hospitalized-isolation compartment to reduce infectious disease. The lower isolation rate (r_1 and r_2) signifies limited healthcare resources in the respective countries. As a whole, by comparing Figure 4(a) and 4(b), it can be observed that the default and Figure 4(b) present similar outcomes in which r_1 exhibits less impact. Conversely, a different propensity was found for Figure 4(c), when compared with the previous two cases, ensuring that r_2 exhibits substantial impact. A reduction in the incidence of infection in country B is observed for a higher isolation rate, r_2. The phase diagram can be analyzed by the varying isolation rate. First, if we presume $r_1 = 0.3$ (*-i) and $r_1 = 0.8$ (*-ii), as can be seen from Figure 4(B), increasing the $r_1$caused the disease to lessen in country A only for lower values of q (yellow-dotted region). Nevertheless, country B in Figure

Preprints (www.preprints.org) | NOT PEER-REVIEWED | Posted: 14 May 2020 doi:10.20944/preprints202005.0242.v1

4(B) shows non-sensitivity along r_1. Yet, when the isolation rate, r_2, is reasonably high, the fraction of infected individuals in country B presents an interesting phenomenon (white-dotted region) that requires further exploration (Figure 4(C)). If the acquired isolation rate r_2 is large, the parameter η_2 is futile. This is theoretically possible, as a higher isolation rate absorbs more isolated people from the infected state, where an individual undergoing hospitalized-isolation reduces further spread. Thus, it appears that a higher isolation rate at the inferior quarantine rate demonstrated lower infected individuals, which, in turn, reduced the risk of the incidence of infection.

Travel restriction

The necessity of modeling an importation-exportation epidemic framework can be understood from the phase diagram for infected individuals in Figure 5. For this purpose, we present line diagrams for infected densities over time in panel A and total infected individuals in an epidemic season (at equilibrium) as a 2D heat-map along with $(\eta, q)-$ phase space in panel B. Here, the sub-panel (a) presents the portion of infected individuals living in country A, which is entirely independent of I_0. Sub-panels (b)–(d) show the infected individuals staying in country B for $I_0 = 0.0, 0.0001,$ and 0.1, respectively. If no traffic between two countries occurs, the neighboring country (country B) has fully shut out infectious disease from the country of origin. Notably, the none zero I_0 at some point incurs a breakout (sub-panel (a)) despite some time-delay being possible. Our results illustrate that travel restrictions cannot be anticipated to control the global expansion of COVID-19 but may delay the rate of infection if adopted during the initial stages of the epidemic spreading (panel A, Figure 5). In the analysis of the phase diagram presented in panel B, we can realize from sub-panel (b) that the fraction of infected individuals in country B presents a completely disease-free equilibrium for $I_0 = 0.0$. However, with respect to sub-panels (c) and (d), we can confirm that introducing even small amounts of I_0 values (0.0001 & 0.1) leads to a pandemic situation in country B. Correspondingly, panel B directly supports the results depicted in panel A. Thus, unless functioning ideally, travel restrictions with a non-zero threshold are ineffective in suppressing an outbreak. However, it may still bring some time delay to an emerging outbreak. The more the threshold for the restriction is introduced, the more time an emerging outbreak can be observed, which can be useful in preparation for an epidemic.

Healthcare resources

Here, we assess the impact of the availability of medical resources to reduce the transmission of COVID-19. In this sense, let us remark that the threshold value of J_0 allows us to change the level of isolation rate (see equation 7) while considering epidemic spreading shown in Figure 6. Panel A represents the line graph of (a) infected individuals and (b) isolated individuals for $J_0 = 0.0, 0.001, 0.01, 0.05, 0.1,$ and 0.5. In addition, panel B indicates the 2D phase diagram along (η, q) −space for (i) $J_0 = 0.0$, (ii) $J_0 = 0.01$, and $J_0 = 0.1$. Throughout, we can see from Figure 6 (panels A and B) that the fraction of infected individuals decreased as the threshold values of J_0 increased. This refers to a well-organized and highly facilitated healthcare system implemented by health authorities being crucial in controlling infectious disease.

Surprisingly, through close observation of panel B in Figure 6, in the case of a lower η and a lower q, a disease-free equilibrium is detected (dotted area). This can be explained as follows. If the medical resources denoted by J_0 become affluent (reaching infinity as an extreme though unrealistic), i.e., $J_0 = 0.1$, the parameter η is counterproductive. This means that quarantine becomes meaningless. It would be conceivable, as sufficiently large medical resources can easily absorb a large number of infected individuals to place in hospitalized-isolation, which is the best approach for suppressing disease transmission in the local community, as patients are not allowed to demonstrate contact with those susceptible to the disease.

 doi:10.20944/preprints202005.0242.v1

Conclusion

Motivated by the ongoing COVID-19 outbreak, we propose the export-importation SEIQJR epidemic model to analyze the impact of quarantine and hospitalized-isolation strategies on the control and preclusion of contagious diseases. Model research and numerical simulations were carried out, considering human mobility effects along with several parameters, such as travel restrictions, medical resources, and public counter-compliancy. We applied the epidemic model to the validation and projection of the propagation of COVID-19 in China, Italy, and the ROK. Through mathematical analysis, we found that the system exhibits two equilibrium points: disease-free for $R_0 < 1$ and an epidemic state for $R_0 > 1$, where R_0 is the basic reproduction number. Aside from the two-body system, the most important contribution is that our model can easily be extended to a general $n-$subpopulations model for other countries.

The present work that utilized natural infectious cases, statistical analysis, theoretical analysis, normalized numerical examination, and the risk of disease importation-exportation to systematically explore the aspects of the COVID-19 epidemic incidence beyond what was previously reported. We observed an established quarantine and hospitalized-isolation policy introduced by the government to be crucial to reducing the spread of the disease when active vaccines or proper treatment is unavailable. Additionally, we found that if the medical resources are severely limited, possible active-provisions to control epidemic transmission are to either quarantine or people's compliance. Also, we observed that although travel restrictions are useful in the early stage of the outbreak when it is still somewhat confined, its benefit may be less effective once the transmission is more widespread. Lastly, we expect that this study will bring attention to the adoption of further controlling strategies by policymakers and constituents.

Acknowledgment

This study was partially supported by Grant-in-Aid for Scientific Research from JSPS, Japan, KAKENHI (Grant No. JP 19KK0262, and JP 20H02314A) awarded to Professor Tanimoto. We would like to express our gratitude to them.

Authors' contributions. K M Ariful Kabir developed the model, performed numerical simulations, analysed results and drafted the manuscript. Atiqur Chowdhury carried out the statistical and analytical analysis to validate the model. Jun Tanimoto helped designing the study, supervised and also helped draft the manuscript.

Competing interests. We declare we have no competing interests.

References

1. World Health Organization. Coronavirus. World Health Organization cited January 19, 2020. Available: https://www.who.int/health-topics/coronavirus.
2. Zhou, P., Yang, X. L., Wang, X. G., Hu, B., Zhang, L., Zhang, W., et al. A pneumonia outbreak associated with a new coronavirus of probable bat origin. Nature. 2020. https://doi.org/10.1038/s41586-020-2012-7.
3. Zhu, N. et al. China Novel Coronavirus Investigating and Research Team, A novel coronavirus from patients with pneumonia in China, 2019. N. Engl. J. Med. 727-733 (2020).
4. Xu, B., et al. Epidemiological data from the COVID-19 outbreak, real-time case information. Sci.Data 7. 106 (2020).
5. Backer, J. A., Klinkenberg, D., Wallinga, J. Incubation period of 2019 novel coronavirus (2019-nCoV) infections among travellers from Wuhan, China, 20-28, Euro Surveill, 25 (2020).
6. Li, Q. Early transmission dynamics in Wuhan, China, of novel coronavirus-infected pneumonia. N. Eng. J. Med. NEJMoa2001316 (2020).

7. Chen, N., Zhou, M., Dong, X., et al. Epidemiological and clinical characteristics of 99 cases of 2019 novel coronavirus pneumonia in Wuhun, China: a descriptive study. Lancet, 395 (10223): 507-13, PMID 32007143, (2020).
8. Huang, C., Wang, Y., Li, X., Ren, L., Zhao, J., Hu, Y., et al. Clinical features of patients infected with 2019 novel coronavirus in Wuhan, China. Lancet. 2020. https://doi.org/10.1016/S0140-6736(20)30183-5.
9. Worldometer (https:// www.worldometers.info/coronavirus/) accessed 20th April, 2020.
10. World Health Organization. No vaccine, specific drug against coronavirus yet: WHO, April 13, 2020. Available: https://www.aa.com.tr/en/health/no-vaccine.
11. Chen, S., Yang, J., Yang, W., Wang, C., Barnighausen, T. COVID-19 control in China during mass population movements at New Year. Lancet 395, 764-766 (2020).
12. Du, Z., Wang, L., Cauchemez, S., Xu, X., Wang, X., Cowling, B. J., Meyers, L. A. Risk for transportation of 2019 novel coronavirus disease from Wuhun to other citiesin China. Emerg. Infect. Dis. 26 (2020).
13. Quilty, B. J., Clifford, S., Flasche, S., Eggo, R. M. CMMID nCoV working group, Effectiveness of airport screening at detecting travellers infected with novel coronavirus (2019-nCoV). Euro Surveill. 25, 2000080 (2020).
14. Hollingsworth, T. D., Ferguson, N. M., Anderson, R. M. Frequent travellers and rate of spread of epidemics. Emerg. Infect. Dis. 13, 1288-1294 (2007).
15. Jun, G., Yu, J., Han, L., Duan, S. The impact of traffic isolation in Wuhan on the spread of 2019-nCov. medRxiv 2020.02.04.20020438. 5 feb, (2020).
16. Chowdhury, A., Kabir, K.A., Tanimoto, J. How quarantine and social-distancing policy can suppress the outbreak of novel coronavirus in developing or under poverty level countries: a mathematical and statistical analysis, doi: 10.21203/rs.3.rs-20294/v1 (2020).
17. Lopez, L. F., Amaku, M., Coutinho, F. A. et al. Modelling Importations and Exportations of infectious diseases via Travellers, Bull Math Bio. 78, 185-209 (2016).
18. Yongzhen, P., Shaoying, L., Shuping, L., Changguo, L. A delayed SEIQR epidemic model with pulse vaccination and the quarantine measure, Comp. and Math. With App. 58, 135-145 (2009).
19. Li, M. Y., Muldowney, J. S. Global stability for the SEIR model in epidemiology, Math. Bio., 125, 155-164 (1995).
20. Feng, Z. Final and Peak Epidemic Sizes for SEIR Models with Quarantine and Isolation. Math. Biosci. Eng. 4, 675-686, (2007).
21. Safi, M. A., Imran, M., Gumel, A. B. Threshold dynamics of a non-autonomous SEIRS model with quarantine and isolation. Theory Biosci. 131, 19-30, (2012).
22. Arenas, A., et al. A mathematical model for the spatiotemporal epidemic spreading of COVID19, medRxiv preprint, https://doi.org10.1101/2020.03.21.20040022.
23. Teles, P. Predicting the evolution of SARS-COVID-2 in Portugal using an adapted SIR model previously used in south korea for the MERS outbreak, arXiv:2003:10047v1[q-bio.PE] 23 var 2020.
24. Chen, Y. C., Lu, P. E., Chang, C. S., Liu, T. H. A time-dependent SIR model for COVID-19 with undetectable infected persons, arXiv:2003:00122v2[q-bio.PE] 30 var 2020.
25. Xia, Z. Q., Zhang, J., Xue, Y. K., Sun, G. Q., Jin, Z. Modeling the transmission of middle east respirator syndrome corona virus in the republic of korea. Plose ONE 10, e0144778 (2015).
26. Canabarro, A., Tenorio, E., Martins, R., Martins, L., Brito, S., Chaves, R.; Data-Driven Study of the the COVID-19 Pandemic via Age-Structured Modelling and Prediction of the Health System Failure in Brazil amid Diverse Intervention Strategies, medRxiv preprint doi: https://doi.org/10.1101/2020.04.03.20052498 (2020).
27. Day, T., Park, A., Madras, N., Gumelm, A., Wu, J. When is quarantine a useful control strategy for emerging infectious diseases? Am. J. Epidemiol. 163, 479-85, (2006).
28. Feng, Z. Final and peak epidemic sizes for SEIR models with quarantine and isolation Math. Biosci. Eng. 4, 675-686, (2007).

29. Giubilini, A., Douglas, T., Maslen, H. Savulescu, J. Quarantine, isolation and the duty of easy rescue in public health. Dev. World Bioeth. 18, 182-189, (2018).
30. Alam, M., Kabir, K. M., Tanimoto, J. Based on mathematical epidemiology and evolutionary game theory, which is more effective: quarantine or isolation policy?. J. Stat. Mech. 03350, (2020).
31. Liangrong, P., Wuyue, Y., Dongyan, Z., Changjing, Z., Liu, H. Epidemic analysis of COVID-19 in China by dynamical modeling, medRxiv, 2020. https://doi.org/10.1101/2020.02.16.20023465
32. Chen, T., Rui, J., Wang, Q., et al. A mathematical model for simulating the phase-based transmissibility of a novel coronavirus. Infect Dis Poverty 9, 24 (2020). https://doi.org/10.1186/s40249-020- 00640-3.
33. Kraemer, M. U. G. et al. The effect of human mobility and control measures on the COVID-19 epidemic in China, Science, 10.1126/abb4218(2020).
34. Wells, C. R., et al. Impact of international travel and border control measures on the global spread of the novel 2019 coronavirus outbreak, pnas, :10.1073/pnas.2002616117 (2020).
35. Kabir, K. M. A., Tanimoto, J. Impact of awareness in metapopulation epidemic model to suppress the infected individuals for different graphs. European Physical Journal B 92, 199, (2019).
36. Keeling, M. J., Bjornstad, O. N.,Grenfell, B. T. "Metapopulation dynamics of infectious diseases" in Ecology, Genetics and evolution of metapopulations, Elsevier 2004, pp.415-445.
37. Watts, D. J., Muhamad, R., Medina, D. C., Dodds, P. S. Multiscale, resurgent epidemics in a hierarchical metapopulation model. Proc. Natl. Acad.Sci.USA, 102, 11157-11162 (2005).
38. Nagatani, T., Ichinose, G., Tainaka, K. Epidemic spreading in unidirectional mobile agents. J. Phys. Soc. Japan, 86, 113001, (2017).
39. Nagatani, T., Ichinose, G., Tainaka, K. Epidemics of random walkers in metapopulation model for complete, cycle and star graphs. Journal of Theo. Biol. 450, 66-75 (2018).
40. Kabir, K. M. A., Tanimoto, J. Evolutionary vaccination game approach in metapopulation migration model with information spreading on different graphs. Chaos Solitons Fractals 120, 41-55 (2019).
41. Kabir, K. M. A., Kuga, K., Tanimoto, J. Analysis of SIR epidemic model with information spreading of awareness. Cha. Sol. & Frac. 119, 118-125 (2019).
42. Kabir, K. M. A., Kuga, K., Tanimoto, J. The impact of information spreading on epidemic vaccination game dynamics in a heterogeneous complex network-A theoretical approach. Cha. Sol. & Frac., 132, 0960-0779 (2020).
43. Kabir, K. M. A., Jusup, M., Tanimoto, J. Behavioral incentives in a vaccination –dilemma setting with optional treatment, PRE, 100, 062402 (2019).

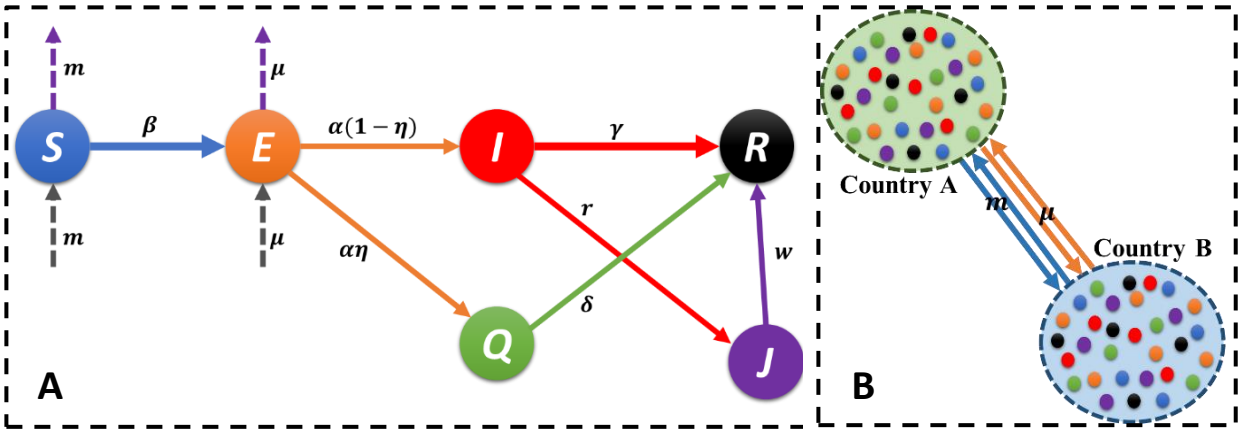

Figure 1. Schematic diagram of (A) the SEIQJR epidemic model and (B) the exportation- importation mechanism.

Preprints (www.preprints.org) | NOT PEER-REVIEWED | Posted: 14 May 2020 doi:10.20944/preprints202005.0242.v1

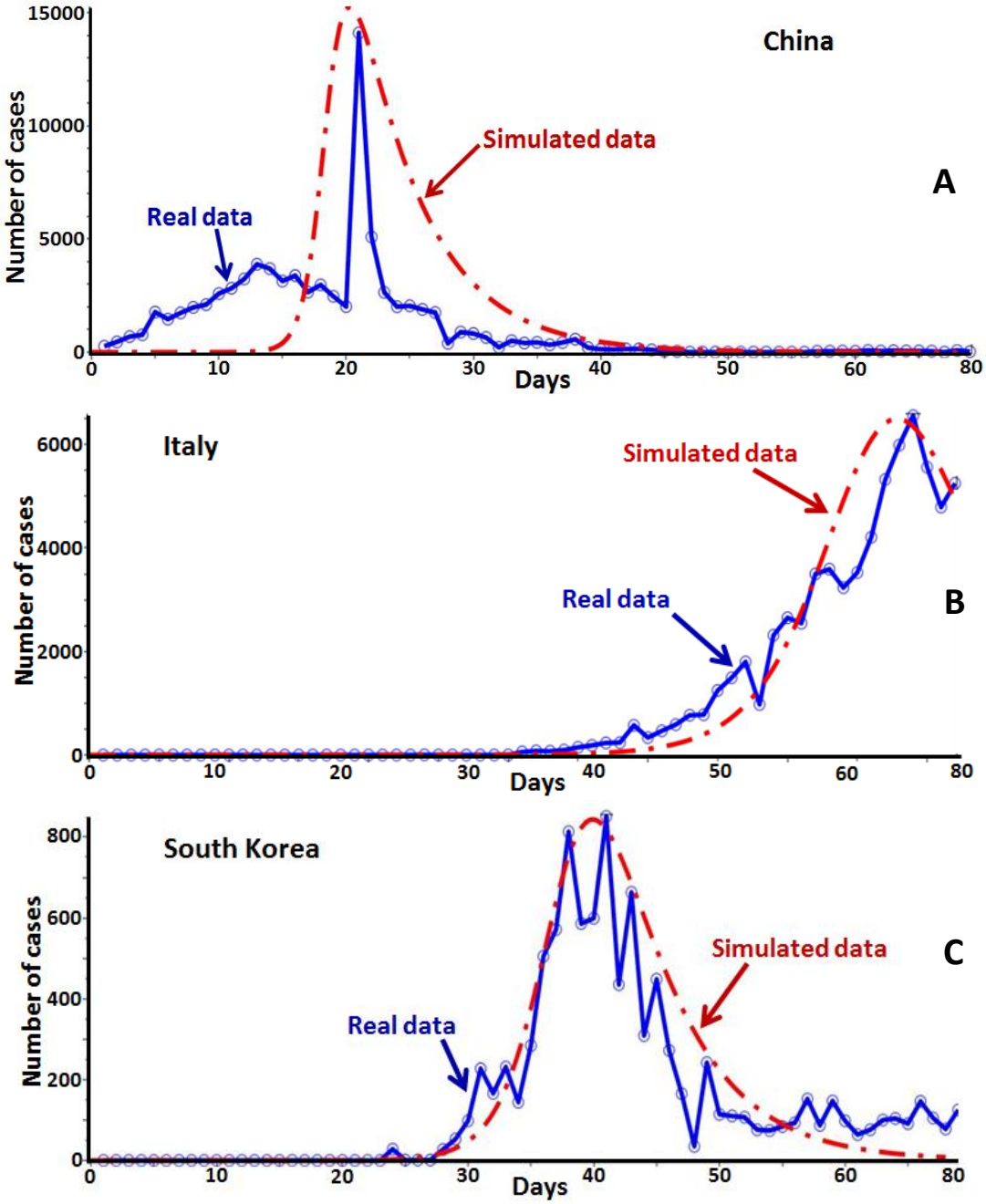

Figure 2. Comparison of the results for each country (A) China, (B) Italy, and (C) the Republic of Korea (ROK) of the SEIQJR epidemic model. The line colored with red corresponds to simulated data, and blue indicates real cases reported [9].

Preprints (www.preprints.org) | NOT PEER-REVIEWED | Posted: 14 May 2020 doi:10.20944/preprints202005.0242.v1

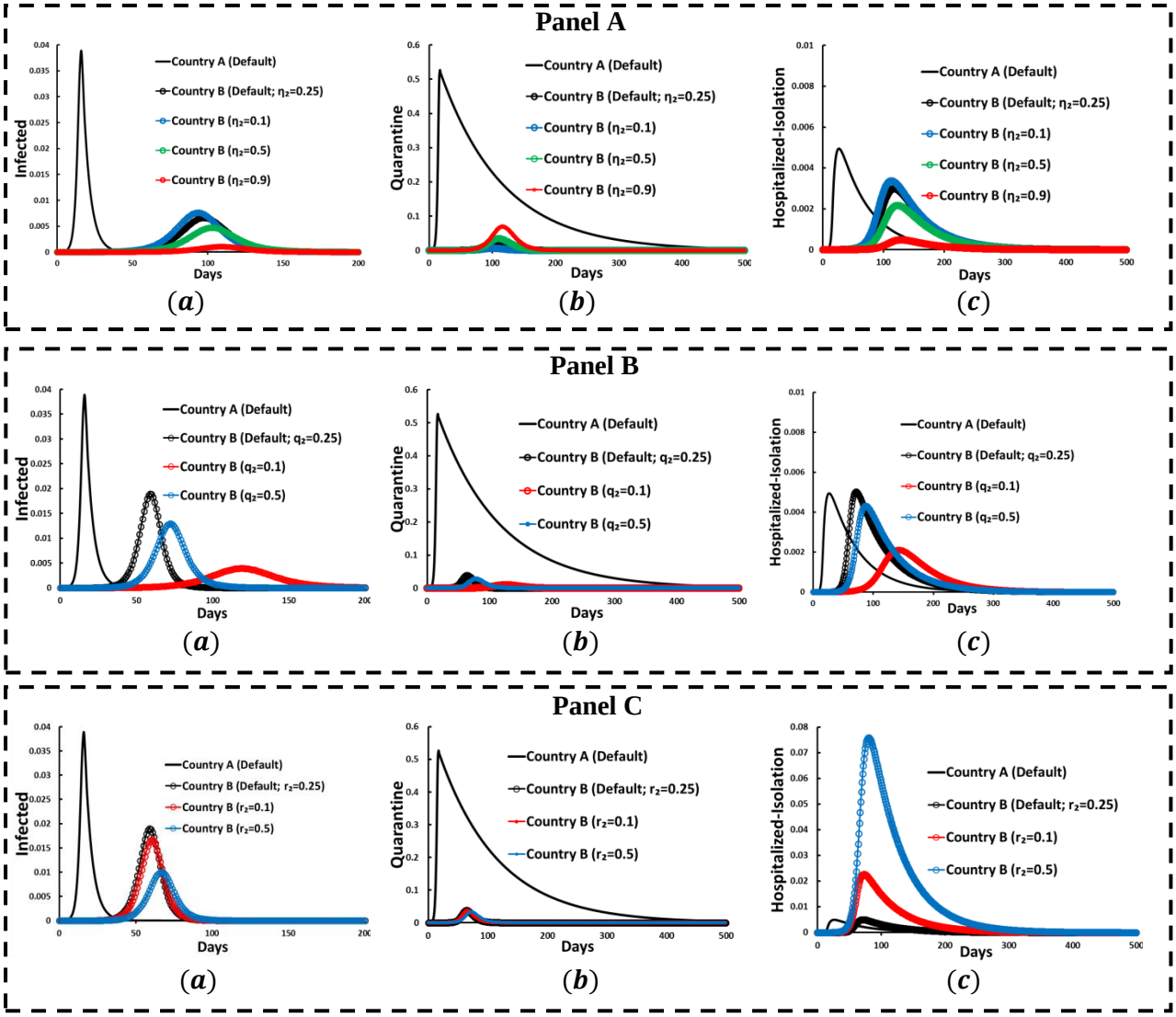

Figure 3. The time sequences of the (a) infected, (b) quarantined, and (c) hospitalized-isolation individuals. Here, panels A, B, and C show the time series of varying parameters η, q, and r, respectively. Other parameter settings are described in Table 2 (the default case). Other values are as follows: $I_0 = 0.02$, and J_0 is infinitely large.

Preprints (www.preprints.org) | NOT PEER-REVIEWED | Posted: 14 May 2020 doi:10.20944/preprints202005.0242.v1

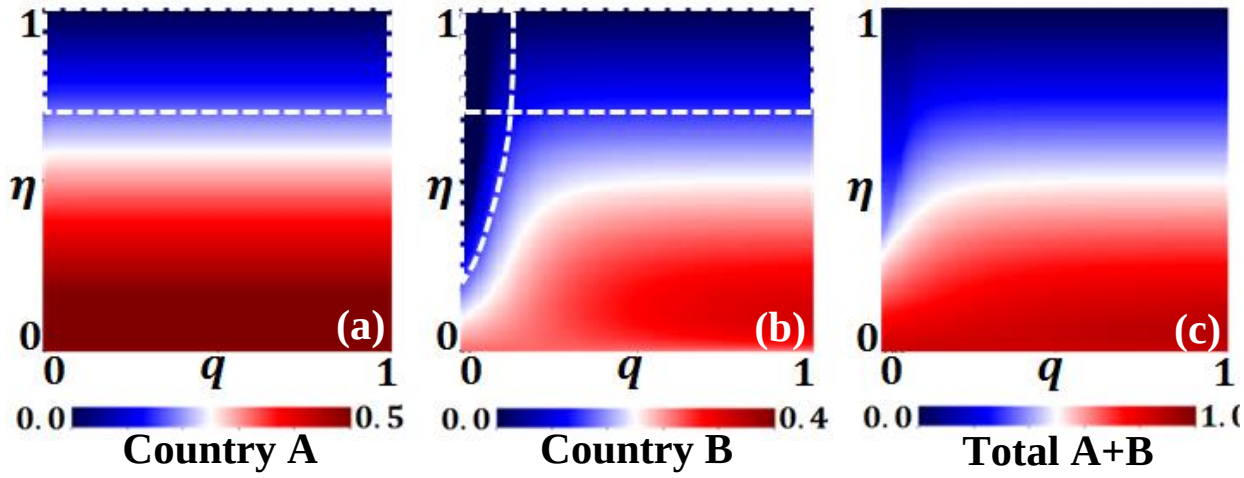

Figure 4 (A). Two-dimensional phase diagram of the infected individuals defined as the "default case" along with the quarantine acquired rate, $\eta_1 = \eta_2 = \eta$, and the public counter-compliant factor, $q_1 = q_2 = q$. Here, (a), (b), and (c) present the infected incidence of country A, country B, and the total of (A + B), respectively. Table 2 is used to build the phase portrayed per the parameter settings with the exclusion of $\eta_1(\eta_2)$ and $q_1(q_2)$. Other values are as follows: $I_0 = 0.02$, and J_0 is infinitely large.

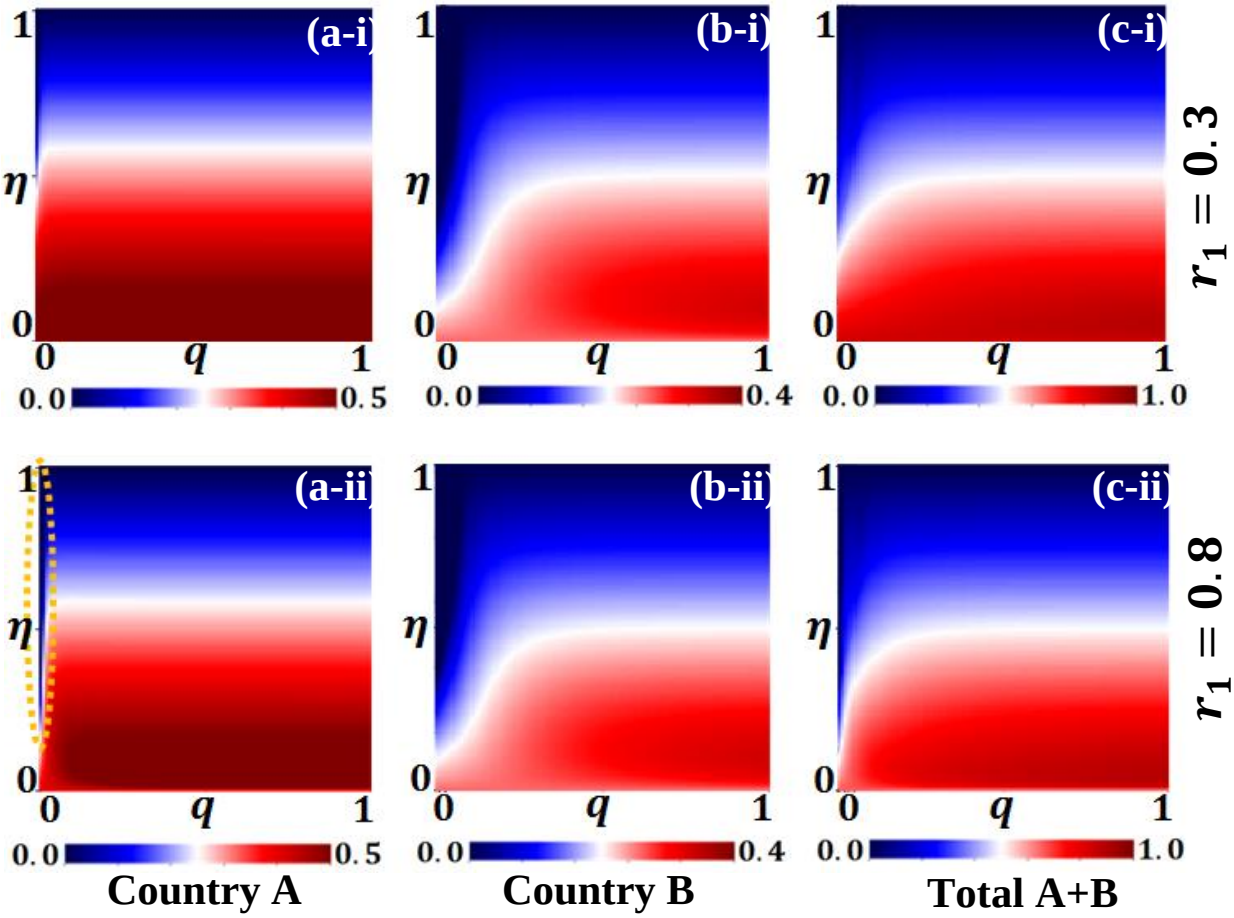

Preprints (www.preprints.org) | NOT PEER-REVIEWED | Posted: 14 May 2020 doi:10.20944/preprints202005.0242.v1

Figure 4 (B). Two-dimensional phase diagram of infected individuals for parameter space $r_1 = 0.3$ and $r_1 = 0.8$ along the quarantine acquired rate, $\eta_1 = \eta_2 = \eta$, and the public counter-compliant factor, $q_1 = q_2 = q$. Here, (a), (b), and (c) present the infected incidence of country A, country B, and the total of (A + B), respectively. Table 2 is used to build the phase portrayed per the parameter settings with the exclusion of $\eta_1(\eta_2)$ and $q_1(q_2)$. Other values are as follows: $I_0 = 0.02$, and J_0 is infinitely large.

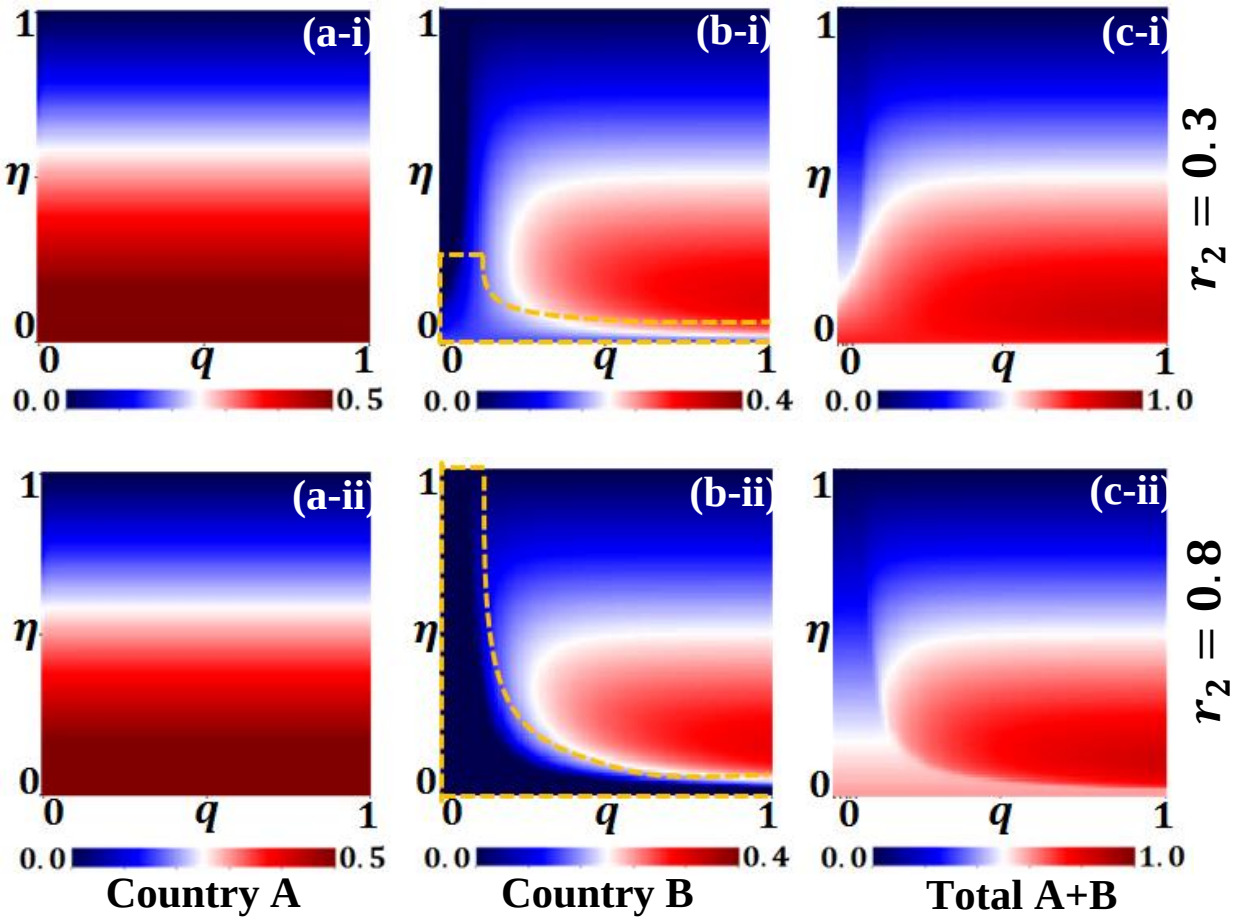

Figure 4 (C). Two-dimensional phase diagram of infected individuals for parameter space $r_2 = 0.3$ and $r_2 = 0.8$ along the quarantine acquired rate, $\eta_1 = \eta_2 = \eta$, and the public counter-compliant factor, $q_1 = q_2 = q$. Here, (a), (b), and (c) present the infected incidence of country A, country B, and the total of (A + B), respectively. Table 2 is used to build the phase portrayed per the parameter settings with the exclusion of $\eta_1(\eta_2)$ and $q_1(q_2)$. Other values are as follows: $I_0 = 0.02$, and J_0 is infinitely large.

Preprints (www.preprints.org) | NOT PEER-REVIEWED | Posted: 14 May 2020 doi:10.20944/preprints202005.0242.v1

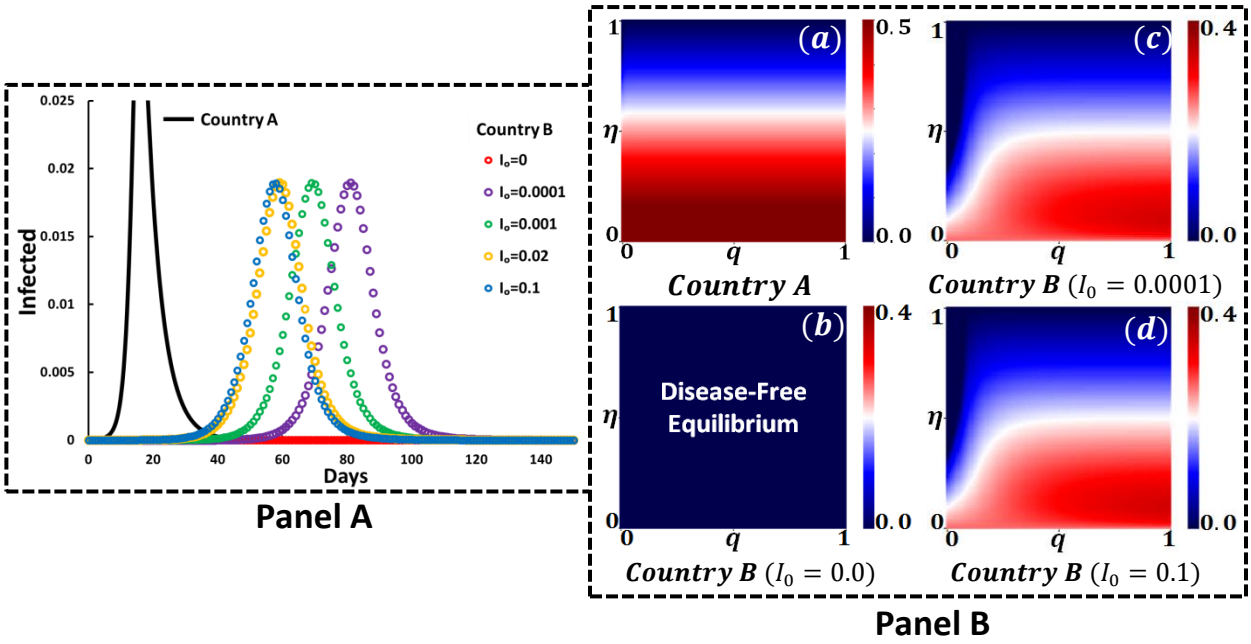

Figure 5. Panel A consists of graphs indicating infected individuals over time where the variation of critical infected densities are $I_0 = 0, 0.0001, 0.001, 0.02$, and 0.1. Panel B indicates the phase diagram of infected individuals for (a) country A (default), (b) country B with $I_0 = 0.0$, (c) country B with $I_0 = 0.0001$, and (d) country B with $I_0 = 0.1$ along η and q. All parameters are chosen from Table 2, and J_0 is infinitely large.

Preprints (www.preprints.org) | NOT PEER-REVIEWED | Posted: 14 May 2020 doi:10.20944/preprints202005.0242.v1

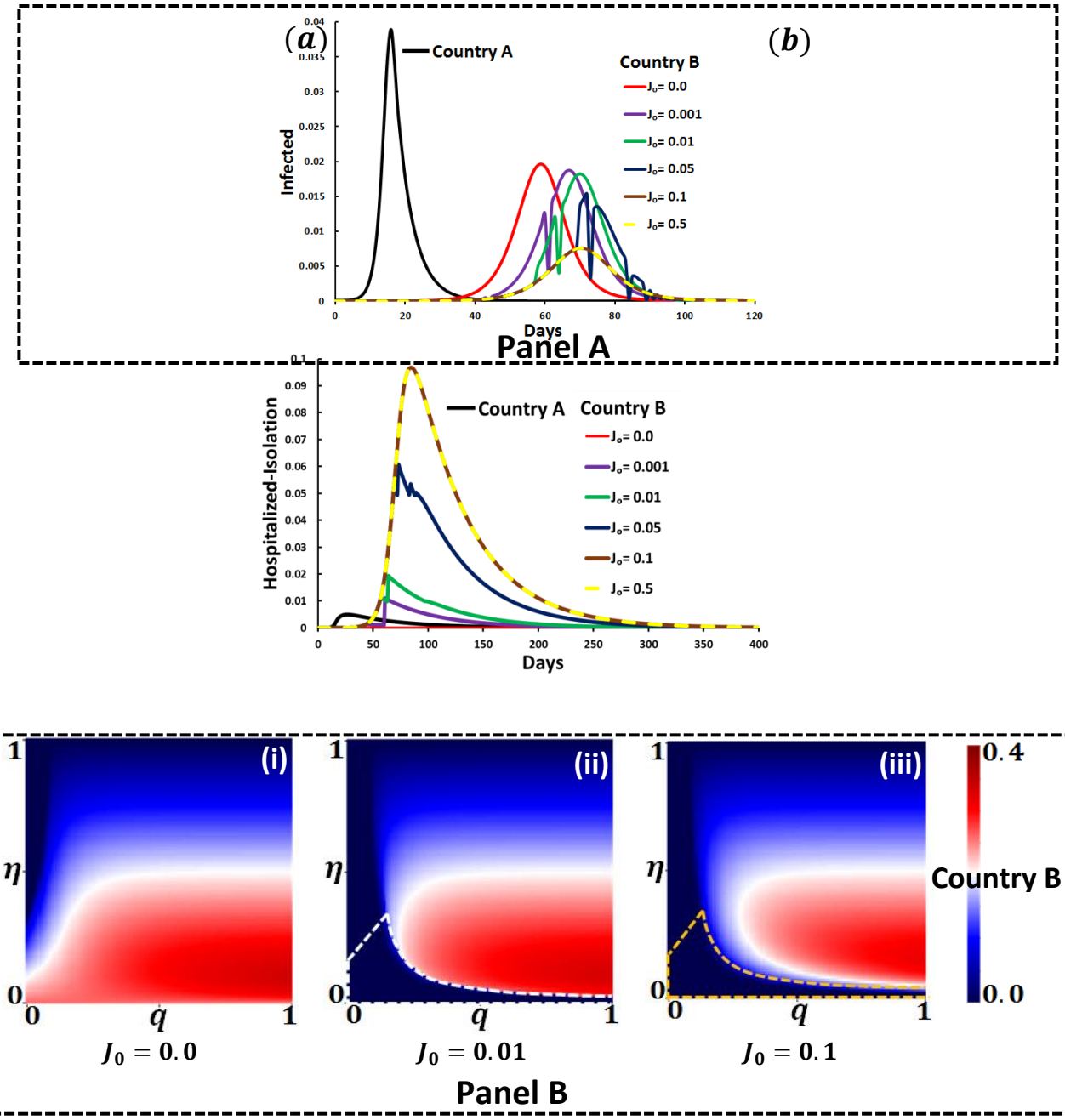

Figure 6. Panel A consists of line graphs indicating (a) infected and (b) isolated individuals over time where the variation of critical J_0 are $0.0, 0.001, 0.01, 0.05, 0.1$, and 0.5. Panel B presents the phase diagrams of infected individuals for country B with (i) $J_0 = 0.0$, (ii) $J_0 = 0.01$, and (iii) $J_0 = 0.1$ along η and q. Rather, all parameters are chosen from Table 2, and $I_0 = 0.02$.

Preprints (www.preprints.org) | NOT PEER-REVIEWED | Posted: 14 May 2020 doi:10.20944/preprints202005.0242.v1

Appendix

Fitting of parameters for China

Model: $524.96 + 1.3991535 \times v - 0.24155837 \times 10^{-4} - 4 \times v^2$

Table A1. Table of fitted parameters for China

	Estimate	Standard error	t-statistic	p-value
Parameter 1	524.9571	568.7250	0.9230	0.3597
Parameter 2	1.3992	0.4389	3.1881	0.0023
Parameter 3	0.0000	0.0000	− 0.6686	0.5063

Here, $R^2 = 0.3470$ and adjusted $R^2 = 0.3252$

Fitting of parameters for Italy

Model: $-75.941 + .71518307 \times v - .67329540 \times 10^{-4} - 4 \times v^2$

Table A2. Table of fitted parameters for China

	Estimate	Standard error	t-statistic	p-value
Parameter 1	−75.9411	66.8979	−1.1352	0.2608
Parameter 2	0.7152	0.1043	6.8601	0.0000
Parameter 3	0.0001	0.0000	3.4648	0.0010

Here, $R^2 = 0.9594$ and adjusted $R^2 = 0.9580$

Fitting of parameters for the Republic of Korea (ROK)

Model: $-11.744 + 1.5036764 \times v.53895667 \times 10^{-3} - 3 \times v^2$

Table A3. Table of fitted parameters for the ROK

	Estimate	Standard error	t-statistic	p-value
Parameter 1	−11.7445	16.3013	−0.7205	0.4740
Parameter 2	1.5037	0.1734	8.6740	0.0000
Parameter 3	−0.0005	0.0002	−2.1972	0.0319

Here, $R^2 = 0.8749$ and adjusted $R^2 = 0.8708$